Published in final edited form as:
J Control Release. 2015 January 10; 0: 48–57. doi:10.1016/j.jconrel.2014.10.026.

Effect of surface chemistry on nanoparticle interaction with gastrointestinal mucus and distribution in the gastrointestinal tract following oral and rectal administration in the mouse

Katharina Maisel[a,b,1], **Laura Ensign**[a,c,1,2], **Mihika Reddy**[a,b], **Richard Cone**[a,d], and **Justin Hanes**[a,b,c,e,2]

[a]Center for Nanomedicine at the Wilmer Eye Institute, Johns Hopkins University School of Medicine, 400 N. Broadway, Baltimore, MD 21231

[b]Department of Biomedical Engineering, Johns Hopkins University School of Medicine, 720 Rutland Avenue, Baltimore, MD 21205

[c]Department of Ophthalmology, The Wilmer Eye Institute, Johns Hopkins University School of Medicine, 400 N. Broadway, Baltimore, MD 21231

[d]Department of Biophysics, Johns Hopkins University, 3400 N. Charles Street, Baltimore, MD 21218

[e]Center for Cancer Nanotechnology Excellence, Institute for NanoBio Technology, Johns Hopkins University, 3400 N Charles Street, Baltimore, MD 21218

Abstract

It is believed that mucoadhesive surface properties on particles delivered to the gastrointestinal (GI) tract improve oral absorption or local targeting of various difficult-to-deliver drug classes. To test the effect of nanoparticle mucoadhesion on distribution of nanoparticles in the GI tract, we orally and rectally administered nano- and microparticles that we confirmed possessed surfaces that were either strongly mucoadhesive or non-mucoadhesive. We found that mucoadhesive particles (MAP) aggregated in mucus in the center of the GI lumen, far away from the absorptive epithelium, both in healthy mice and in a mouse model of ulcerative colitis (UC). In striking contrast, water absorption by the GI tract rapidly and uniformly transported non-mucoadhesive mucus-penetrating particles (MPP) to epithelial surfaces, including reaching the surfaces between villi in the small intestine. When using high gavage fluid volumes or injection into ligated intestinal loops, common methods for assessing oral drug and nanoparticle absorption, we found that both MAP and MPP became well-distributed throughout the intestine, indicating that the barrier properties of GI mucus were compromised. In the mouse colorectum, MPP penetrated into

[2]Correspondence: Laura Ensign, PhD lensign@jhmi.edu, or Justin Hanes, PhD, hanes@jhmi.edu, 443-287-7921, 400 N. Broadway St., 6th Floor, Baltimore, MD 21231.
[1]Authors contributed equally to the work presented in this article

mucus in the deeply in-folded surfaces to evenly coat the entire epithelial surface. Moreover, in a mouse model of UC, MPP were transported preferentially into the disrupted, ulcerated tissue. Our results suggest that delivering drugs in non-mucoadhesive MPP is likely to provide enhanced particle distribution, and thus drug delivery, in the GI tract, including to ulcerated tissues.

Keywords

Drug delivery; nanoparticles; colon; inflammatory bowel disease (IBD); ulcerative colitis; mucus penetrating particles

Introduction

More than 80% of drugs are taken orally, making the gastrointestinal (GI) tract the primary site of drug delivery [1-3]. Many potent small molecule drugs are hydrophobic and poorly water soluble, which often translates into poor oral bioavailability [1]. Micronization of hydrophobic drugs to increase surface area is a common method to improve drug dissolution, thereby enhancing uptake of poorly soluble drugs [1, 4-6]. Encapsulation within polymer nano-and microparticles is another approach that has been demonstrated to improve oral delivery of many types of drugs, ranging from small molecules to large proteins [1, 2, 7]. However, whether a poorly soluble drug is micronized into a suspension of hydrophobic particulates, or any drug is encapsulated within conventional polymeric nanoparticles, the final product is typically a hydrophobic particle that is strongly adhesive to mucus [8].

Current dogma suggests that mucoadhesion of particulates is beneficial for maximizing delivery in the GI tract. Mucoadhesion purportedly allows the particulates to leave the chyme by adhering to the mucus layers lining the GI tract [8-10]. It is widely agreed that enhanced drug delivery from the chyme to the entire (highly-folded) GI tract epithelium, including the highly absorptive jejunum, where fluid absorption greatly speeds nutrient uptake, is desired for maximum absorption into the systemic circulation [8, 11-14]. Furthermore, for treating diseases of the colorectum, such as ulcerative colitis (UC), and for preventing rectal transmission of sexually transmitted infections (STI), rectal, rather than oral administration, may be more effective [15-18].

However, GI tract mucus is a continuously secreted barrier that traps and coats foreign particulates and pathogens to protect the underlying epithelium [8]. Thus, we recently suggested that it is possible that the rapid clearance of the most superficial luminal mucus layers in the GI tract may limit the effectiveness of mucoadhesive particles [8]. Mucoadhesive nano- and microparticulate formulations have been shown to significantly improve delivery of several drug molecules in the GI tract compared to drugs administered without a delivery system, at least partly by increasing drug solubility, providing sustained release, and protecting the drug cargo. However, it has yet to be carefully tested whether mucoadhesive nano- and microparticles provide advantages over non-mucoadhesive particles in terms of partitioning from the chyme into the GI mucus layers. It also has not been established which type of particle provides the most uniform distribution over the absorptive epithelium in the GI tract.

In this paper, we sought to directly test the GI distribution of particles that were carefully confirmed to possess either strongly mucoadhesive or non-mucoadhesive surfaces. We hypothesized that particles smaller than the mucus mesh spacing and with non-mucoadhesive surfaces would penetrate the thick mucus barrier in the GI tract, leading to a more uniform delivery of the particles to the absorptive epithelium in healthy animals. We also tested these particle types in an animal model of ulcerative colitis (UC), a subset of inflammatory bowel disease (IBD) characterized by disruption of the epithelial barrier, increased mucus secretion, and increased inflammation, with the hypothesis that the non-mucoadhesive particles may more effectively penetrate through the mucus barrier and enter into the diseased tissues of the GI tract.

To test our hypotheses, we prepared nanoparticles of various sizes that possessed either unmodified hydrophobic surfaces, or hydrophilic, neutrally charged surfaces obtained via a dense coating with polyethylene glycol (PEG). We first confirmed in mouse GI mucus *ex vivo* that the unmodified nanoparticles were mucoadhesive (mucoadhesive particles, MAP), whereas the PEG-coated particles were non-mucoadhesive (mucus-penetrating particles, MPP). Subsequently, we administered MAP and MPP to mice by oral gavage, ligated intestinal loops and by rectal enema, and observed their distribution in the jejunum, ileum, and colon. We further compared MAP and MPP distribution in inflamed regions of the small intestine and the associated ulcerated colonic tissue regions in two common mouse models of UC.

Materials and Methods

Animal model

Female 6-8 week old CF-1 mice were purchased from Harlan (Indianapolis, IN). Mice were placed on liquid diet for 24 h and starved for 24 h to produce reduced amounts of softer, more human-like feces, as opposed to the dry, hard pellets normally produced by mice. To induce TNBS-colitis, mice were anesthetized with isoflurane and dosed rectally with 0.125 mg/g of 2,4,6-trinitrobenzenesulfonic acid (TNBS, also known as picrylsulfonic acid, Sigma-Aldrich) in 50% ethanol as previously described [19]. To induce DSS-colitis, mice were given 4% w/v dextran sulfate sodium (DSS, Sigma-Aldrich) in their drinking water for four days, as previously described [20]. Only mice that lost at least 5% of their body weight, a common measure of disease induction, were used [19]. These procedures reliably produced mice with colorectal tissue with clear signs of inflammation, including thickening of the mucosa and loose stool. Mice with DSS- and TNBS-induced colitis were allowed access to food and water ad libitum. All procedures were approved by the Johns Hopkins Animal Care and Use Committee.

Nanoparticle formulation

Fluorescent, carboxylate-modified polystyrene nanoparticles (PS-COOH) of various sizes (40 nm, 100 nm, 200 nm, 500 nm) were purchased from Molecular Probes (Eugene, OR) and used as model conventional mucoadhesive particles (MAP). To produce mucus-penetrating particles (MPP), PS-COOH nanoparticles were densely coated with polyethylene glycol) (PEG), as previously described [21]. Briefly, 5 kDa methoxy-PEG-

amine (Creative PEGworks), N-Hydroxysulfosuccinimide (Sigma), and 1-Ethyl-3-(3-dimethylaminopropyl) carbodiimide (EDC, Invitrogen) were dissolved in 200 mM borate buffer and added to PS-COOH to facilitate coupling of carboxylic acid and amine groups. Nanoparticle size was characterized using dynamic light scattering (90° scattering angle), and ζ-potential was determined via laser Doppler anemometry with a Zetasizer Nano ZS90 (Malvern Instruments, Southborough, MA) (Table S1). We have previously found that a near-neutral ζ-potential for these particles indicates that the surface is sufficiently coated with PEG to rapidly penetrate human cervicovaginal mucus (Table S1) [22]. All measurements were performed at 25°C and according to instrument settings.

Nanoparticle distribution in the mouse small intestine and colorectum

Nanoparticles were diluted to 0.2 - 0.02% w/v in water for distribution studies depending on particle size and mode of administration. For nanoparticle distribution in the small intestine, 50 μl of nanoparticles suspended in deionized (DI) water were administered via oral gavage. Sections of the jejunum were excised 1 h (colitis) and 2 h (healthy) post administration, and sections of the ileum were excised 6 h post administration and subsequently flash frozen in Optimal Cutting Temperature compound (OCT). For intestinal loop experiments, animals were anesthetized with avertin solution, and the ileum was exposed from a small incision in the abdomen. A 2 cm region was tied off using surgical sutures, and 200 μl of fluid was injected into the loop using a syringe. The loops were excised 30 min after administration of nanoparticles and frozen in OCT. To assess colorectal distribution, nanoparticles were suspended in DI water as an enema vehicle. For transverse sections, 20 μl of nanoparticle solution was administered to mice under isoflurane anesthesia. After 5-10 min, their colorectal tissues were excised and immediately frozen in OCT. For all tissues, sections were cut 6 μm thick using a Leica CM-3050-S cryostat. The tissue sections were briefly fixed in 10% formalin, air dried, and stained with ProLong Gold antifade reagent with 4′,6-diamidino-2-phenylindole (DAPI). Sections were imaged using an inverted epifluroescence microscope (Zeiss Axio Observer).

For surface coverage measurements in the jejunum, 50 μl of nanoparticles suspended in DI water were administered via oral gavage, and tissues removed after 2 h. The tissues were then sliced open longitudinally and flattened between two glass slides to expose the epithelial folds (colon) or villi (jejunum), as previously described [23]. For surface coverage measurements in the colorectum, mice were given a 200 μl DI water enema prior to nanoparticle administration to remove remaining pellets and ensure maximum tissue surface exposure. After 10 min, to ensure that all excess enema fluid was either expelled or absorbed by the epithelium, 50 μl of nanoparticle solution was administered rectally, and the tissues were excised within 5-10 min. Tissues were imaged using an inverted epifluroescence microscope (Zeiss Axio Observer). Control tissues (mice receiving no nanoparticles) were imaged to determine tissue background fluorescence levels to ensure that the fluorescent nanoparticle signal was above background. For quantification, 6 images were obtained at regular intervals along the tissue surface. The images were threshholded and the % coverage was quantified using ImageJ as previously described [23]. Data represents the average for n ≥ 3 mice ± the standard error of the mean.

Ex vivo tracking of nanoparticles in small intestinal and colorectal mucus of mice

Mice were prepared as described above. On day 3 after TNBS treatment (UC colon) or after 3 days of liquid diet and a 24 h starvation period (healthy small intestine), *ex vivo* tracking experiments were performed as previously described [22, 24]. Briefly, the small intestine or colorectum was excised, longitudinally sliced open, and a 1 cm segment of tissue was placed in a custom-made 0.5 × 1 cm chamber. A volume of 0.5 μL of nanoparticles of various sizes (diluted to 0.02-0.08% w/v) was carefully pipetted on top of the mucus coating the tissues. The wells were then sealed by placing a cover slide was on top of the tissue and affixing it using superglue. Movies were obtained using an inverted epifluorescence microscope with a 100×/1.46 NA oil-immersion objective. Movies were taken using an EMCCD camera (Evolve 512; Photometrics) for 20 s at temporal resolution of 66.7 ms. Nanoparticle positional data was obtained using Metamorph software and the resulting trajectories were analyzed using MATLAB. At least 100 nanoparticles of each size and type were tracked for 50 frames or more to obtain nanoparticle mean square displacements (MSD) as a function of timescale calculated as $\langle \Delta r^2(\tau) \rangle = [x(t+\tau)-x(t)]^2 + [y(t+\tau)-y(t)]^2$ [24-27]. Our prior work has found that static error can be estimated to be 20 nm, much smaller than the size of the nanoparticle displacements [25, 28].

Results

Distribution of orally-administered MAP and MPP in the small intestines of healthy mice

We first performed *ex vivo* multiple particle tracking (MPT) experiments, as previously described [22], to confirm that our model mucoadhesive particles (MAP) were adhesively trapped in mucus layers coating freshly excised mouse small intestine tissue. The trajectories of 200 nm MAP indicated adhesive immobilization (Fig 1A). In contrast, the trajectories of similarly-sized MPP indicated that MPP freely diffused in the mucus layers coating mouse small intestine tissue (Fig 1A). We then sought to determine whether adhesive interactions with small intestine mucus would impact nanoparticle delivery following oral administration by gavage. We used small gavage fluid volume (50 μL) to administer MAP and MPP to minimize volume-related artifacts [29]. As shown in Figure 1B, adhesion of MAP to luminal mucus layers resulted in exclusion of these particles from most of the epithelial surface (black in the image). In contrast, MPP were found distributed over much more of the epithelial surface, such that the impression of the flattened villus tips could be visualized to be nearly completely surrounded by MPP (Fig 1B). We then quantified the epithelial surface area covered by nanoparticles, and found that MPP covered 74 ± 4% of the epithelial surface of the jejunum, compared to only 35 ± 7% by MAP (Fig 1C).

Using the same oral administration methods, we then examined the cross-sectional distribution of the particles. We found that the adhesive MAP were clumped together in the lumen of the jejunum and ileum, unable to penetrate between the villi (Fig 2). In contrast, MPP distributed evenly throughout the tissue in both the jejunum and ileum, even though a small gavage fluid volume was used (Fig 2).

Impact of fluid volume and mode of administration on MAP and MPP distribution in the small intestines of healthy mice

One challenge with interpreting and comparing literature reports of oral administration of nano-and microparticles is that the experimental protocols often differ significantly. We thus investigated the effects of fed state, administration method (oral gavage vs. intestinal loop), and gavage fluid volume on the GI distribution of MAP and MPP. Animals are almost always starved prior to oral administration experiments to avoid the confounding changes in transit time and absorption attributable to varied GI content. As shown in Figure 3A, not only was there little apparent effect on intestinal distribution of MPP after oral gavage to mice in the “fed” state, but the difference in distribution between co-administered MAP and MPP appeared even more pronounced in the fed state compared to the starved state. In the area close to the lumen (L), outlined at 10× magnification by a pink box and then shown at 20×, MAP were found in large aggregates sometimes colocalized with some MPP, whereas MPP were also dispersed between the villi. In the area far from the lumen and among the villi, outlined at 10× magnification by a yellow box and then shown at 20×, MAP were essentially absent in the villi, whereas MPP were dispersed throughout and between the villi (Fig 3A). Thus, in the fed state, in contrast to MAP, non-adhesive MPP appeared to leave the digesta, penetrate the entire mucus barrier, and become well distributed on the epithelial surfaces.

We next investigated whether the high fluid volumes often used with intestinal loops or oral gavage can impact the distribution of MAP or MPP. We anticipated that administering particles in a large volume of fluid, that can distend the intestines and potentially cause viscous fingering through the mucus barrier [8], would enhance MAP distribution throughout the small intestine. As expected, filling the intestine with fluid containing MAP in an ileal loop model led to dispersion of MAP throughout the intestine and between the villi (Fig 3B). The distribution of MAP was very similar to MPP administered to intestinal loops (Fig S1). Similarly, when we administered MAP by oral gavage in 5-fold higher fluid volume (250 μL), although MAP appeared to aggregate to some extent, they became distributed in the jejunum and ileum as though the mucus barrier was not present (Fig 3B). Overall, the small intestine distributio n of MAP in an intestinal loop model, and after high volume gavage of MAP (that would be impractic al to scale to humans), was very similar to distributio n of MPP, and was in stark contrast to the distributio n of MAP administe red by gavage in low fluid volume (Fig 2).

Distribution of MAP and MPP in the colorectum of healthy mice

Prior to *in vivo* experiments to investigate MAP and MPP distribution in the colorectum of healthy mice following administration by enema, we first confirmed that MAP, regardless of particle diameter, were adhesively trapped in the mucus layers coating colorectal tissues freshly prepared *ex vivo*, whereas MPP <230 nm in diameter rapidly diffused through mouse colorectal mucus, as indicated by their trajectories (Fig 4). With this confirmation, we compared MAP and MPP distribution on the colonic epithelium when administered a hypotonic enema vehicle that causes osmotically-induced fluid absorption by the colonic tissue and, thus, fluid advection toward the epithelium [22]. MAP were trapped and aggregated within colorectal mucus *in vivo* regardless of particle size, leading to limited

distribution to only select areas in the colorectal lumen (Fig 4). In contrast, MPP uniformly coated the epithelial surface of the colorectum within only a few minutes after administration. MPP 40 nm and 100 nm in size reached all of the deep, folded surfaces, evenly coating the colorectal epithelium (Fig 4). MPP 200 and 500 nm in size also provided improved distribution compared to similarly sized MAP (Fig 4). However, 200 and 500 nm MPP did not distribute throughout the colorectal epithelium as uniformly as 40 and 100 nm MPP (Fig 4), a result consistent with the rapid diffusion of 40 and 100 nm MPP observed by *ex vivo* multiple particle tracking on freshly excised mouse GI tissue.

We then sought to quantify the colorectal distribution of MAP and MPP in the mouse colorectum after administration by hypotonic enema. MAP of all sizes were found to associate with luminal mucus bundles (Fig 5A), limiting the apparent colorectal surface coverage of 40, 100, 200 and 500 nm MAP to 39 ± 4%, 38 ± 2%, 38 ± 3%, and 36 ± 3%, respectively (Fig 5B). In contrast, MPP reached more of the colorectal tissue surface, with overall surface coverage decreasing as particle size increased (Fig 5A). MPP 40 nm in size provided a nearly uniform coating of the colorectal tissue surface (84 ± 1%), and while a significant portion of 100 nm MPP reached the tissue surface (leading to 80 ± 1% coverage of the colorectal surface), some 100 nm MPP remained in the luminal mucus gel (Fig 5A). MPP with diameters of 200 and 500 nm MPP were also found on the colorectal tissue surface (76 ± 2% and 55 ± 3% of the tissue surface, respectively; Fig 5B), however, an increasing amount appeared to be associated with the luminal mucus plug as MPP size increased (Fig 5A). Penetration of colorectal mucus by larger MPP was likely hindered by steric interactions with the mouse colorectal mucus mesh as MPP size increased, which is consistent with what we have observed using *ex vivo* MPT (Fig 4 and [22]), as well as with the cross-sectional colorectal MPP distribution observed in Figure 4.

MAP and MPP transport in colorectal mucus from mice with TNBS-induced colitis

Mucus hypersecretion and degradation is associated with UC, which may impact the structure of the mucus mesh and potentially alter the relative adhesive character of MAP or non-adhesive character of MPP. Thus, we first used MPT to quantify the transport of MAP and MPP in colorectal mucus on freshly excised *ex vivo* colorectal tissue obtained from mice with TNBS-induced colitis. The ensemble-averaged mean square displacement (<MSD>) of MAP in UC mouse colorectal mucus was >8,000-fold less than the theoretical MSD of similarly sized nanoparticles in water, regardless of size, indicating adhesive immobilization (Fig 6A). In contrast, MPP up to 200 nm in size readily diffused in colorectal mucus from mice with UC. Steric trapping of 500 nm MPP was observed in UC colorectal mucus, resulting in a low <MSD> that was similar to all sizes of MAP (Fig 6A). The distribution of the individual particle MSD values indicated that 100 nm MPP were uniformly diffusive, and >30% of 200 nm MPP diffused rapidly in UC colorectal mucus (Fig 6B). The <MSD> of 100 and 200 nm MPP in UC mucus were 2- and 25-fold increased, respectively, in UC colorectal mucus compared to in colorectal mucus from healthy mice (Table 1), indicating an increase in the overall pore size in UC colorectal mucus compared to healthy mouse colorectal mucus.

Distribution of MAP and MPP in the GI tract of mice with induced colitis

After confirming that MAP were adhesively immobilized in GI mucus from mice with UC, while MPP were diffusive, we sought to evaluate the distribution of MAP and MPP in the colorectum of mice with UC. Similar to the distribution observed in the healthy mouse colorectum, MAP of all sizes were adhesively trapped in mucin bundles in the colorectum of mice with TNBS-induced UC, thus limiting distribution over the tissue surface (Fig 7A). Mucin bundling induced by MAP also trapped some MPP that were co-administered with MAP, as evidenced by the low amount of individual MAP compared to co-localized MAP and MPP, and MPP alone (Fig 7A). Regardless, MPP of all sizes distributed over more of the colorectal tissue surface in both healthy mice and mice with UC (Fig 7A). There was an increase in the colorectal surface coverage by 200 nm MPP in mice with UC compared to in healthy mice (Fig 7A), which is consistent with the increase in the fraction of diffusive 200 nm MPP observed in UC mucus compared to in healthy colorectal mucus in the *ex vivo* MPT experiments (Fig 6B).

We next sought to test whether inflammation in the small intestine associated with IBD would impact the distribution of MAP and MPP after oral administration, but TNBS-induced colitis only locally affects the colorectum. It is generally accepted that DSS-induced colitis causes inflammation and mucus hypersecretion in the small intestine [20], so we used this model of induced colitis to observe nanoparticle distribution in the inflamed small intestine after oral administration. Inflammation was evident by the lack of organized alignment of cell nuclei and general damage to the small intestine villi compared to healthy mice. We found that, similar to our findings in healthy mice, 200 nm MAP aggregated in the lumen of the inflamed small intestinal regions, whereas MPP distributed throughout and between the villi (Fig 7B), following oral administration.

UC is also characterized by increased epithelial permeability and ulceration, such that nanoparticle uptake into the tissue has been hypothesized as a mechanism for improved and selective nanoparticle-based drug delivery to treat UC [30-35]. We hypothesized that the ability of MPP to penetrate the mucus barrier would lead to increased accumulation of MPP compared to MAP in the tissue ulcerations. As shown in Figure 8, co-administration of MAP and MPP to mice by enema provided a stark visual contrast between the aggregated and poorly distributed MAP compared to the evenly distributed MPP in the healthy mouse colorectum, regardless of nanoparticle size. A similar contrast in colorectal distribution was seen for MAP and MPP in the colorectum of mice with TNBS-induced UC, and MPP also penetrated into damaged areas of the epithelium (Fig 8, green arrows) much more efficiently than MAP. MAP were also found near damaged areas of the epithelium, but tended to aggregate in the mucus or adhere only to the outer cell layer (Fig 8, red arrows).

Discussion

Enhancing the uniformity and proximity of drug-loaded particulates to the absorptive regions of the GI epithelium may improve both systemic drug absorption and local drug delivery for disorders such as IBD. Since most small molecule drugs are hydrophobic, strategies such as drug micronization and encapsulation within micro- or nanoparticle systems are used to overcome solubility limitations, leading to enhanced drug absorption [1,

2, 4-6, 8]. However, additional barriers to effective drug absorption in the GI tract exist, such as the mucus barrier lining the GI tract. Mucus can form multiple low-affinity interactions with particulate matter, including hydrophobic interactions, such that most types of drug particles and polymer particles stick to it [8, 36-39]. There are many other mechanisms by which mucoadhesion occurs, including electrostatic interactions and polymer interpenetration [36, 38, 40, 41], and these systems are all designed to facilitate strong adhesion to mucus. We demonstrated here that conventional hydrophobic mucoadhesive particles (MAP) stick to mucus and digesta, resulting in aggregation and limited distribution throughout the GI tract after oral and rectal administration. In contrast, non-mucoadhesive particles that penetrate through small and large intestine mucus (MPP) were able to reach nearly the entire tissue surface, which is likely to provide improved drug delivery for both local and systemic applications.

Mucoadhesion, which is generally defined as the interaction between a biological or synthetic material and the mucosa [42], is widely employed for drug delivery to mucosal surfaces. For example, mucoadhesion of pharmaceutical devices to surfaces that experience constant physical stress and drug clearance on the order of seconds to minutes, such as the buccal or ocular surfaces, can markedly improve drug delivery [43]. Also, devices generally larger in size than the thickness of the mucus barrier, such as micropatches [44, 45] and large microspheres functionalized with silicon nanowires [46], may be able to interact directly with the underlying mucosa to increase residence time in the GI tract. The distinction between *mucus* adhesion and *mucosa* adhesion is very important, and size scale is one factor that determines the efficiency by which a system designed to stick to the mucosal epithelium may contact the epithelium, as opposed to becoming trapped in the mucus gel instead. This paper shows that a typical mucoadhesive micro- or nanoparticle adheres to the luminal mucus gel before reaching the mucosa, thereby limiting particle distribution in the GI tract, and likely limiting GI residence time to the minutes to hours it takes for the mucus barrier to clear [8, 36]. It is not known at present whether MAP or MPP would be retained longer in the GI tract. However, our other work in the lung [47] and vagina [23] demonstrated that MPP enter more slowly cleared mucus layers, leading to prolonged retention of MPP compared to MAP that stick to the luminal mucus layers (note that MAP were called conventional particles, or “CP”, in these other papers). Carefully comparing the GI tract residence time of MAP and MPP will likely require the use of larger animals with GI transit times more similar to humans, such as dogs and pigs [48]. In rodents, the rapid GI transit time and production of a succession of hard, desiccated pellets (we have observed that mice produce a pellet once every 5-10 min) limits the ability to correlate particle retention in the rodent GI tract to what would be expected in humans. Assessing GI tract retention in a more physiologically relevant animal model is a high priority for future development of MPP for GI tract drug delivery.

It is important to recognize that numerous examples of mucoadhesive micro- and nanoparticle systems exist that provided improved drug delivery compared to the unencapsulated drug. For proteins where mucoadhesive particle systems have provided significantly improved bioavailability, such as insulin [49-53] and calcitonin [51, 54-56], encapsulation within the nanoparticle core shields the cargo from degradation in the harsh

GI environment and can provide sustained release, which likely account for the enhanced protein uptake. However, while drug delivery to the GI tract via mucoadhesive particles may provide significant advantages compared to administration of unencapsulated drug, our work suggests that the extent of the advantage is limited by particle aggregation and adhesion to mucus *in vivo*. In other work, liposomes coated with a commonly used polymer for mucoadhesive formulations, chitosan, were shown to aggregate in simulated GI fluid *in vitro*, and provided decreased cyclosporine A bioavailability *in vivo* compared to unmodified liposomes [57]. Also, the percentage of drug that was absorbed by GI tissues was increased when the mucus barrier was degraded prior to oral administration, and without an intact mucus barrier, drug delivery was improved for chitosan liposomes compared to unmodified liposomes [57]. Similarly, incubating invasin-coated PS nanoparticles in porcine mucin prior to oral administration led to decreased systemic absorption in rats [58]. Cell culture studies have also demonstrated decreased uptake of mucoadhesive nanoparticles in the presence of mucus [8, 59]. Indeed, we demonstrate here that MAP, in contrast to MPP, tend to aggregate in the GI tract lumen, where they are largely restricted from accessing the absorptive epithelium in the small intestine (both by poor surface coverage of the epithelium and by not penetrating to obtain close proximity to the epithelium). Our results suggest that drug delivery to the GI tract could be further improved by using non-mucoadhesive nanoparticles that distribute throughout the GI tract and reach nearly the entire epithelial surface. Definitive illustration of such improvement will await future studies seeking to test whether an improvement in systemic drug absorption will result from the increased access of drug in MPP to the absorptive epithelium, and/or improved efficacy of local drug treatment from increased uniformity of drug delivery to the affected tissues and cells.

We also demonstrate that methods commonly used for testing mucoadhesive particle systems may obscure the importance of the mucus barrier in the GI tract. For example, intestinal loop models have been used for decades to investigate systemic absorption of nanoparticles and drugs. In this model, a portion of the small intestine is excised from the abdominal cavity, thread is used to tie off the ends to make an isolated “loop”, and the test solution of interest is directly infused into the segment of intestine. The intestine is then placed back into the abdominal cavity, and absorption is allowed to occur over several hours. Using this model, as much as 67% of mucoadhesive nanoparticles were found in the blood and various organs, indicating systemic absorption [60]. However, as we demonstrate here, administering fluid into a tied-off loop distends the intestine and dilutes the mucus barrier, distributing MAP throughout the entire intestinal segment in a manner indistinguishable from MPP. Other studies have also demonstrated elevated absorption of nanoparticles after oral gavage. For example, more than 30% of 500 nm polystyrene nanoparticles were absorbed after oral gavage in one study [60]. However, the gavage volume used is important, as similar dilution effects can occur when large fluid volumes are gavaged to rodents. For example, Eyles *et al.* demonstrated that, with the same amount of 870 nm PS particles in each dose, a 5-fold increase in gavage volume from 0.1 mL to 0.5 mL in rats also caused a 5-fold increase in the percentage of nanoparticles found in the bloodstream [29]. Thus, when we administered MAP by gavage in 5-fold higher volume of fluid (0.25 mL as opposed to 0.05 mL for the rest of our studies), it is perhaps not surprising

that the small intestinal distribution of MAP was indistinguishable from MPP. For most oral drug delivery systems, including pills, the driving force for absorption would not be large volumes of fluid forced into the intestines, but rather the natural digestive absorption processes, and we demonstrate here that MPP have a clear advantage over MAP in being drawn through the mucus barrier with the fluid as it is absorbed. We further demonstrated that the stark contrast between the small intestinal distribution of MAP and MPP was further enhanced when the nanoparticles were co-administered in the fed state. Nutrients that can penetrate the mucus barrier are transported to the epithelium by the rapid absorption of water by the GI tract. This 'advective' transport by the flow of water rapidly transports nutrients into the highly infolded surfaces between villi. Water absorption increases in the fed state, increasing the speed of this advective transport process, and MPP take advantage of this process for efficient and uniform drug delivery. In contrast, MAP stick to the outer layers of mucus and aggregate in clumps in the center of the lumen, far from the epithelial surface.

For certain applications, such as rectal protection against sexually transmitted diseases with microbicides or treatment of UC, colorectal drug delivery may be preferable [18, 61-63]. Our work indicates that, when administered locally to the colorectum via enema, MPP of all sizes tested provided improved distribution over the epithelial surface compared to MAP. The hypotonic enema vehicle caused fluid absorption by the colorectal epithelium, thus advectively transporting MPP, but not MAP, through pores in the mucus mesh to reach the epithelial surface. We had previously observed similar results for MAP compared to MPP in the mouse vagina following administration in hypotonic aqueous vehicles [22].

UC has been associated with mucus hypersecretion and a reduction in mucus barrier properties [31, 32, 64]. Using MPP of various sizes, we showed that local inflammation in the TNBS-induced UC mouse model altered the structure of colorectal mucus, allowing larger (200 nm) MPP to penetrate more efficiently compared to penetration in healthy mouse colorectal mucus. However, despite the reduction in steric barrier properties, colorectal mucus in TNBS-induced UC maintained adhesivity toward MAP. It has been demonstrated in animal models of IBD that mucoadhesive nanoparticles preferentially accumulate in inflamed areas of the GI tract due to increased mucus accumulation and potentially phagocytosis by macrophages [33, 65]. In addition to mucus gel hypersecretion, inflammation is associated with breakdown of the adherent mucus layer in the colon, which normally excludes bacteria in the healthy colon [66], leading to bacterial infiltration into the tissue [67, 68]. Increased tissue permeability may be a mechanism for selective particle uptake and retention in highly inflamed regions; indeed, a measureable decrease in epithelial resistance was observed in tissue biopsies obtained from patients with IBD compared to healthy controls, which led to accumulation of mucoadhesive particles (microparticles > nanoparticles) in ulcerated tissue regions [69]. The accumulation increased with increasing disease severity, but the accumulation was typically less than 1% of the field of view [69]. It was then demonstrated with Ussing chambers and tissue biopsies that chitosan-modified poly(lactic-*co*-glycolic acid) (PLGA) nanoparticles had even less penetration into tissue from IBD patients compared to PLGA nanoparticles [70]. In contrast, PEG-modified PLGA nanoparticles were found in the tissue specimens in greater amounts [70]. Ussing chamber

models may be limited by the fact that the tissue and mucus are soaked in media; however, our *in vivo* results in a mouse model of UC confirmed that only small amounts of MAP penetrate into ulcerated tissue regions, whereas MPP penetrate the mucus and enter the ulcerated tissue regions in much greater amounts. Importantly, the use of a hypotonic enema vehicle likely enhanced MPP penetration into ulcerated tissue regions throughout the entire colorectum.

Conclusion

We systematically compared mucoadhesive nanoparticle (MAP) and non-mucoadhesive nanoparticle (mucus-penetrating particles, or MPP) behavior in the GI tract of mice. We showed that the mucus barrier strongly limited the distribution and proximity of MAP to epithelial surfaces in both the small and large intestine. In contrast, MPP evenly coated the epithelial surfaces of the GI tract, achieved close contact to the underlying epithelium, and penetrated much more effectively into inflamed regions of UC tissues. Thus, the formulation of drugs into MPP may provide significant advantages in GI retention and drug absorption (owing to increased retention, distribution and proximity to the epithelium). In addition, unlike the clear difference of distribution between MAP and MPP when orally or rectally delivered, MPP and MAP distribute similarly when administered directly to the small intestine, as done in intestinal loop models, or in a high volume of gavage fluid. This indicates that care must be taken when choosing experimental methods for evaluating nanoparticle delivery to the GI tract, as some techniques are not representative of normal GI tract transit. Future studies will determine whether the improved mucosal distribution in the GI tract observed with non-mucoadhesive particles may lead to improved local drug treatments for diseases such as UC and colon cancer, improved microbicide-based protection against sexually transmitted infections, and/or improved oral absorption of drugs.

Supplementary Material

Refer to Web version on PubMed Central for supplementary material.

Acknowledgments

We thank the animal husbandry staff at Johns Hopkins, the Wilmer Microscopy and Imaging Core Facility (grant # EY001765). This work was supported by NIH grants R33AI094519 (J.H., R.C., L.M.E.) and R33AI079740 (J.H., R.C.), the Johns Hopkins University Center for AIDS Research P30AI094189 (L.M.E.), the W.W. Smith Charitable Trust (L.M.E.), and the NSF graduate research fellowship program (K.M.). The mucus penetrating particle technology is being developed by Kala Pharmaceuticals. Dr. Hanes is a co-founder of Kala. Drs. Hanes and Cone own company stock, which is subject to certain restrictions under University policy.

References

1. Gomez-Orellana I. Strategies to improve oral drug bioavailability. Expert Opin Drug Deliv. 2005; 2:419–433. [PubMed: 16296764]
2. Cai Z, Wang Y, Zhu LJ, Liu ZQ. Nanocarriers: a general strategy for enhancement of oral bioavailability of poorly absorbed or pre-systemically metabolized drugs. Curr Drug Metab. 2010; 11:197–207. [PubMed: 20384585]
3. Roger E, Lagarce F, Garcion E, Benoit JP. Biopharmaceutical parameters to consider in order to alter the fate of nanocarriers after oral delivery. Nanomedicine (Lond). 2010; 5:287–306. [PubMed: 20148639]

4. Chaumeil JC. Micronization: a method of improving the bioavailability of poorly soluble drugs. Methods Find Exp Clin Pharmacol. 1998; 20:211–215. [PubMed: 9646283]
5. McInnes GT, Asbury MJ, Ramsay LE, Shelton JR, Harrison IR. Effect of micronization on the bioavailability and pharmacologic activity of spironolactone. J Clin Pharmacol. 1982; 22:410–417. [PubMed: 7130430]
6. Farinha A, Bica A, Tavares P. Improved bioavailability of a micronized megestrol acetate tablet formulation in humans. Drug Dev Ind Pharm. 2000; 26:567–570. [PubMed: 10789071]
7. Hunter AC, Elsom J, Wibroe PP, Moghimi SM. Polymeric particulate technologies for oral drug delivery and targeting: a pathophysiological perspective. Nanomedicine. 2012; 8(Suppl 1):S5–20. [PubMed: 22846372]
8. Ensign LM, Cone R, Hanes J. Oral drug delivery with polymeric nanoparticles: the gastrointestinal mucus barriers. Adv Drug Deliv Rev. 2012; 64:557–570. [PubMed: 22212900]
9. Thanou M, Verhoef JC, Junginger HE. Oral drug absorption enhancement by chitosan and its derivatives. Adv Drug Deliv Rev. 2001; 52:117–126. [PubMed: 11718935]
10. Duran-Lobato M, Munoz-Rubio I, Holgado MA, Alvarez-Fuentes J, Fernandez-Arevalo M, Martin-Banderas L. Enhanced cellular uptake and biodistribution of a synthetic cannabinoid loaded in surface-modified poly(lactic-co-glycolic acid) nanoparticles. J Biomed Nanotechnol. 2014; 10:1068–1079. [PubMed: 24749401]
11. Steffansen B, Nielsen CU, Brodin B, Eriksson AH, Andersen R, Frokjaer S. Intestinal solute carriers: an overview of trends and strategies for improving oral drug absorption. European journal of pharmaceutical sciences : official journal of the European Federation for Pharmaceutical Sciences. 2004; 21:3–16. [PubMed: 14706808]
12. Hamman JH, Demana PH, Olivier EI. Targeting receptors, transporters and site of absorption to improve oral drug delivery. Drug target insights. 2007; 2:71–81. [PubMed: 21901064]
13. Gupta S, Kesarla R, Omri A. Formulation Strategies to Improve the Bioavailability of Poorly Absorbed Drugs with Special Emphasis on Self-Emulsifying Systems. ISRN pharmaceutics. 2013; 2013:848043. [PubMed: 24459591]
14. Thomas VH, Bhattachar S, Hitchingham L, Zocharski P, Naath M, Surendran N, Stoner CL, El-Kattan A. The road map to oral bioavailability: an industrial perspective. Expert opinion on drug metabolism & toxicology. 2006; 2:591–608. [PubMed: 16859407]
15. Frei P, Biedermann L, Manser CN, Wilk M, Manz M, Vavricka SR, Rogler G. Topical therapies in inflammatory bowel disease. Digestion. 2012; 86(Suppl 1):36–44. [PubMed: 23051725]
16. Leyva FJ, Bakshi RP, Fuchs EJ, Li L, Caffo BS, Goldsmith AJ, Ventuneac A, Carballo-Dieguez A, Du Y, Leal JP, Lee LA, Torbenson MS, Hendrix CW. Isoosmolar enemas demonstrate preferential gastrointestinal distribution, safety, and acceptability compared with hyperosmolar and hypoosmolar enemas as a potential delivery vehicle for rectal microbicides. AIDS Res Hum Retroviruses. 2013; 29:1487–1495. [PubMed: 23885722]
17. Carballo-Dieguez A, Bauermeister J, Ventuneac A, Dolezal C, Mayer K. Why rectal douches may be acceptable rectal-microbicide delivery vehicles for men who have sex with men. Sex Transm Dis. 2010; 37:228–233. [PubMed: 19959973]
18. Li J, Chen C, Cao XN, Wang GH, Hu JB, Wang J. Efficacy of topical versus oral 5-aminosalicylate for treatment of 2,4,6-trinitrobenzene sulfonic acid-induced ulcerative colitis in rats. J Huazhong Univ Sci Technolog Med Sci. 2014; 34:59–65. [PubMed: 24496680]
19. Lohr K, Sardana H, Lee S, Wu F, Huso DL, Hamad AR, Chakravarti S. Extracellular matrix protein lumican regulates inflammation in a mouse model of colitis. Inflamm Bowel Dis. 2012; 18:143–151. [PubMed: 21484968]
20. Yazbeck R, Howarth GS, Butler RN, Geier MS, Abbott CA. Biochemical and histological changes in the small intestine of mice with dextran sulfate sodium colitis. J Cell Physiol. 2011; 226:3219–3224. [PubMed: 21351101]
21. Nance EA, Woodworth GF, Sailor KA, Shih TY, Xu Q, Swaminathan G, Xiang D, Eberhart C, Hanes J. A dense poly(ethylene glycol) coating improves penetration of large polymeric nanoparticles within brain tissue. Science Translational Medicine. 2012; 4:149ra119.

22. Ensign LM, Hoen TE, Maisel K, Cone RA, Hanes JS. Enhanced vaginal drug delivery through the use of hypotonic formulations that induce fluid uptake. Biomaterials. 2013; 34:6922–6929. [PubMed: 23769419]
23. Ensign LM, Tang BC, Wang YY, Tse TA, Hoen T, Cone R, Hanes J. Mucus-penetrating nanoparticles for vaginal drug delivery protect against herpes simplex virus. Science Translational Medicine. 2012; 4:138ra179.
24. Lai SK, Hanes J. Real-time multiple particle tracking of gene nanocarriers in complex biological environments. Methods Mol Biol. 2008; 434:81–97. [PubMed: 18470640]
25. Suh J, Wirtz D, Hanes J. Real-time intracellular transport of gene nanocarriers studied by multiple particle tracking. Biotechnology progress. 2004; 20:598–602. [PubMed: 15059007]
26. Dawson M, Krauland E, Wirtz D, Hanes J. Transport of polymeric nanoparticle gene carriers in gastric mucus. Biotechnology progress. 2004; 20:851–857. [PubMed: 15176891]
27. Dawson M, Wirtz D, Hanes J. Enhanced viscoelasticity of human cystic fibrotic sputum correlates with increasing microheterogeneity in particle transport. J Biol Chem. 2003; 278:50393–50401. [PubMed: 13679362]
28. Kim AJ, Boylan NJ, Suk JS, Hwangbo M, Yu T, Schuster BS, Cebotaru L, Lesniak WG, Oh JS, Adstamongkonkul P, Choi AY, Kannan RM, Hanes J. Use of single-site-functionalized PEG dendrons to prepare gene vectors that penetrate human mucus barriers. Angew Chem Int Ed Engl. 2013; 52:3985–3988. [PubMed: 23460577]
29. Eyles J, Alpar O, Field WN, Lewis DA, Keswick M. The transfer of polystyrene microspheres from the gastrointestinal tract to the circulation after oral administration in the rat. J Pharm Pharmacol. 1995; 47:561–565. [PubMed: 8568621]
30. Coco R, Plapied L, Pourcelle V, Jerome C, Brayden DJ, Schneider YJ, Preat V. Drug delivery to inflamed colon by nanoparticles: comparison of different strategies. Int J Pharm. 2013; 440:3–12. [PubMed: 22820482]
31. Fiocchi C. Inflammatory bowel disease: etiology and pathogenesis. Gastroenterology. 1998; 115:182–205. [PubMed: 9649475]
32. Bruewer M, Samarin S, Nusrat A. Inflammatory bowel disease and the apical junctional complex. Ann N Y Acad Sci. 2006; 1072:242–252. [PubMed: 17057204]
33. Lamprecht A, Schafer U, Lehr CM. Size-dependent bioadhesion of micro- and nanoparticulate carriers to the inflamed colonic mucosa. Pharm Res. 2001; 18:788–793. [PubMed: 11474782]
34. Lamprecht A, Ubrich N, Yamamoto H, Schafer U, Takeuchi H, Maincent P, Kawashima Y, Lehr CM. Biodegradable nanoparticles for targeted drug delivery in treatment of inflammatory bowel disease. J Pharmacol Exp Ther. 2001; 299:775–781. [PubMed: 11602694]
35. Lamprecht A, Yamamoto H, Takeuchi H, Kawashima Y. Nanoparticles enhance therapeutic efficiency by selectively increased local drug dose in experimental colitis in rats. J Pharmacol Exp Ther. 2005; 315:196–202. [PubMed: 15980057]
36. Lai SK, Wang YY, Hanes J. Mucus-penetrating nanoparticles for drug and gene delivery to mucosal tissues. Adv Drug Deliv Rev. 2009; 61:158–171. [PubMed: 19133304]
37. Ensign LM, Schneider C, Suk JS, Cone R, Hanes J. Mucus penetrating nanoparticles: biophysical tool and method of drug and gene delivery. Adv Mater. 2012; 24:3887–3894. [PubMed: 22988559]
38. Cone RA. Barrier properties of mucus. Adv Drug Deliv Rev. 2009; 61:75–85. [PubMed: 19135107]
39. Cone, RA. Mucosal Immunology. 3rd. 2005. Mucus; p. 49-72.
40. Peppas NA, Huang Y. Nanoscale technology of mucoadhesive interactions. Adv Drug Deliv Rev. 2004; 56:1675–1687. [PubMed: 15350296]
41. Peppas NA. Molecular calculations of poly(ethyleneglycol) transport across a swollen poly(acrylic acid) mucin interface. J Biomat Sci-Polym E. 1998; 9:535–542.
42. Yoncheva K, Gomez S, Campanero MA, Gamazo C, Irache JM. Bioadhesive properties of pegylated nanoparticles. Expert Opin Drug Deliv. 2005; 2:205–218. [PubMed: 16296748]
43. Serra L, Domenech J, Peppas NA. Engineering design and molecular dynamics of mucoadhesive drug delivery systems as targeting agents. Eur J Pharm Biopharm. 2009; 71:519–528. [PubMed: 18976706]

44. Gupta V, Hwang BH, Lee J, Anselmo AC, Doshi N, Mitragotri S. Mucoadhesive intestinal devices for oral delivery of salmon calcitonin. J Control Release. 2013; 172:753–762. [PubMed: 24035976]
45. Shen Z, Mitragotri S. Intestinal patches for oral drug delivery. Pharm Res. 2002; 19:391–395. [PubMed: 12033369]
46. Uskokovic V, Lee PP, Walsh LA, Fischer KE, Desai TA. PEGylated silicon nanowire coated silica microparticles for drug delivery across intestinal epithelium. Biomaterials. 2012; 33:1663–1672. [PubMed: 22116000]
47. Suk JS, Kim AJ, Trehan K, Schneider CS, Cebotaru L, Woodward OM, Boylan NJ, Boyle MP, Lai SK, Guggino WB, Hanes J. Lung gene therapy with highly compacted DNA nanoparticles that overcome the mucus barrier. J Control Release. 2014; 178:8–17. [PubMed: 24440664]
48. Kararli TT. Comparison of the gastrointestinal anatomy, physiology, and biochemistry of humans and commonly used laboratory animals. Biopharmaceutics & drug disposition. 1995; 16:351–380. [PubMed: 8527686]
49. Wang Y, Zhang X, Cheng C, Li C. Mucoadhesive and enzymatic inhibitory nanoparticles for transnasal insulin delivery. Nanomedicine (Lond). 2014; 9:451–464. [PubMed: 24910876]
50. Momoh MA, Kenechukwu FC, Nnamani PO, Umetiti JC. Influence of magnesium stearate on the physicochemical and pharmacodynamic characteristics of insulin-loaded Eudragit entrapped mucoadhesive microspheres. Drug Deliv. 2014
51. Bakhru SH, Furtado S, Morello AP, Mathiowitz E. Oral delivery of proteins by biodegradable nanoparticles. Adv Drug Deliv Rev. 2013; 65:811–821. [PubMed: 23608641]
52. Furtado S, Abramson D, Burrill R, Olivier G, Gourd C, Bubbers E, Mathiowitz E. Oral delivery of insulin loaded poly(fumaric-co-sebacic) anhydride microspheres. Int J Pharm. 2008; 347:149–155. [PubMed: 17707601]
53. Carino GP, Mathiowitz E. Oral insulin delivery. Adv Drug Deliv Rev. 1999; 35:249–257. [PubMed: 10837700]
54. Takeuchi H, Sugihara H. Absorption of calcitonin in oral and pulmonary administration with polymer-coated liposomes. Yakugaku Zasshi. 2010; 130:1135–1142. [PubMed: 20823671]
55. Makhlof A, Werle M, Tozuka Y, Takeuchi H. A mucoadhesive nanoparticulate system for the simultaneous delivery of macromolecules and permeation enhancers to the intestinal mucosa. J Control Release. 2011; 149:81–88. [PubMed: 20138935]
56. Sinsuebpol C, Chatchawalsaisin J, Kulvanich P. Preparation and in vivo absorption evaluation of spray dried powders containing salmon calcitonin loaded chitosan nanoparticles for pulmonary delivery. Drug Des Devel Ther. 2013; 7:861–873.
57. Chen D, Xia D, Li X, Zhu Q, Yu H, Zhu C, Gan Y. Comparative study of Pluronic((R)) F127-modified liposomes and chitosan-modified liposomes for mucus penetration and oral absorption of cyclosporine A in rats. Int J Pharm. 2013; 449:1–9. [PubMed: 23583840]
58. Hussain N, Florence AT. Utilizing bacterial mechanisms of epithelial cell entry: Invasin-induced oral uptake of latex nanoparticles. Pharmaceut Res. 1998; 15:153–156.
59. Behrens I, Pena AI, Alonso MJ, Kissel T. Comparative uptake studies of bioadhesive and non-bioadhesive nanoparticles in human intestinal cell lines and rats: the effect of mucus on particle adsorption and transport. Pharm Res. 2002; 19:1185–1193. [PubMed: 12240945]
60. Reineke JJ, Cho DY, Dingle YT, Morello AP 3rd, Jacob J, Thanos CG, Mathiowitz E. Unique insights into the intestinal absorption, transit, and subsequent biodistribution of polymer-derived microspheres. Proc Natl Acad Sci U S A. 2013; 110:13803–13808. [PubMed: 23922388]
61. Safdi M, DeMicco M, Sninsky C, Banks P, Wruble L, Deren J, Koval G, Nichols T, Targan S, Fleishman C, Wiita B. A double-blind comparison of oral versus rectal mesalamine versus combination therapy in the treatment of distal ulcerative colitis. Am J Gastroenterol. 1997; 92:1867–1871. [PubMed: 9382054]
62. Marteau P, Probert CS, Lindgren S, Gassul M, Tan TG, Dignass A, Befrits R, Midhagen G, Rademaker J, Foldager M. Combined oral and enema treatment with Pentasa (mesalazine) is superior to oral therapy alone in patients with extensive mild/moderate active ulcerative colitis: a randomised, double blind, placebo controlled study. Gut. 2005; 54:960–965. [PubMed: 15951542]

63. Andreoli A, Spinella S, Levenstein S, Prantera C. 5-ASA enema versus oral sulphasalazine in maintaining remission in ulcerative colitis. The Italian journal of gastroenterology. 1994; 26:121–125. [PubMed: 7914759]

64. Mankertz J, Schulzke JD. Altered permeability in inflammatory bowel disease: pathophysiology and clinical implications. Curr Opin Gastroenterol. 2007; 23:379–383. [PubMed: 17545772]

65. Ulbrich W, Lamprecht A. Targeted drug-delivery approaches by nanoparticulate carriers in the therapy of inflammatory diseases. J R Soc Interface. 2010; 7(Suppl 1):S55–66. [PubMed: 19940000]

66. Johansson MEV, Phillipson M, Petersson J, Velcich A, Holm L, Hansson GC. The inner of the two Muc2 mucin-dependent mucus layers in colon is devoid of bacteria. P Natl Acad Sci USA. 2008; 105:15064–15069.

67. Johansson MEV, Gustafsson JK, Sjoberg KE, Petersson J, Holm L, Sjovall H, Hansson GC. Bacteria Penetrate the Inner Mucus Layer before Inflammation in the Dextran Sulfate Colitis Model. Plos One. 2010; 5

68. Schultsz C, van den Berg FM, ten Kate FW, Tytgat GNJ, Dankert J. The intestinal mucus layer from patients with inflammatory bowel disease harbors high numbers of bacteria compared with controls. Gastroenterology. 1999; 117:1089–1097. [PubMed: 10535871]

69. Schmidt C, Lautenschlaeger C, Collnot EM, Schumann M, Bojarski C, Schulzke JD, Lehr CM, Stallmach A. Nano- and microscaled particles for drug targeting to inflamed intestinal mucosa-A first in vivo study in human patients. Journal of Controlled Release. 2013; 165:139–145. [PubMed: 23127508]

70. Lautenschlager C, Schmidt C, Lehr CM, Fischer D, Stallmach A. PEG-functionalized microparticles selectively target inflamed mucosa in inflammatory bowel disease. Eur J Pharm Biopharm. 2013; 85:578–586. [PubMed: 24084650]

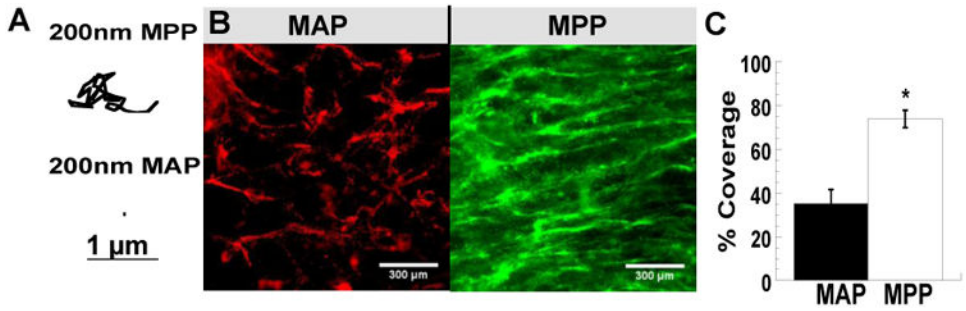

Figure 1. Distribution of MAP and MPP in the jejunum after low volume oral gavage

(A) Trajectories representative of 3 s of movement of 200 nm MAP and MPP in mucus on freshly excised mouse small intestine tissue. (B) Distribution of 200 nm MAP and MPP on flattened mouse jejunum tissues after oral administration. (C) Quantified surface coverage of 200 nm MAP and MPP on flattened mouse jejunum tissue. Images are representative of n ≥ 3 mice. White scale bars indicate 300 µm. Data are calculated as means ± SEM. **P* < 0.05 as compared to CP, Students t-test.

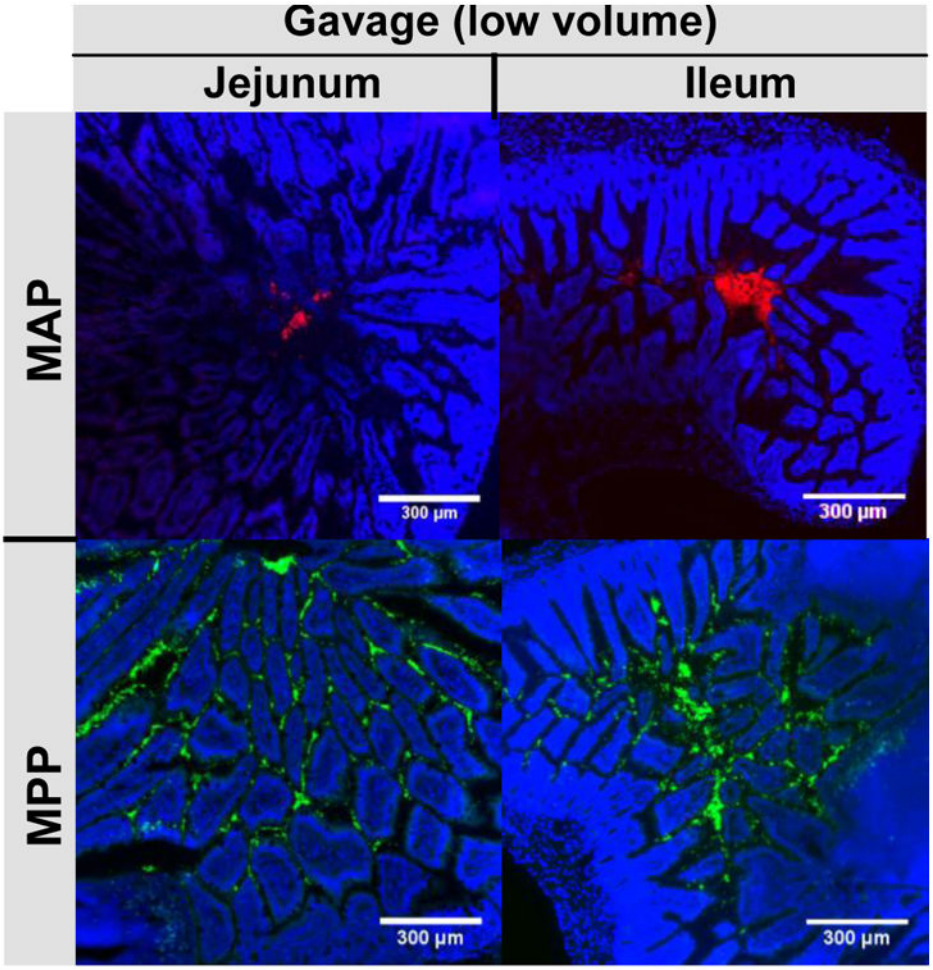

Figure 2. Distribution of MAP and MPP in the jejunum and ileum after low volume oral gavage

Distribution of fluorescent 200 nm MAP or MPP in the healthy mouse jejunum and ileum after low volume oral gavage. White scale bars indicate 300 μm. Images are representative of n ≥ 3 mice.

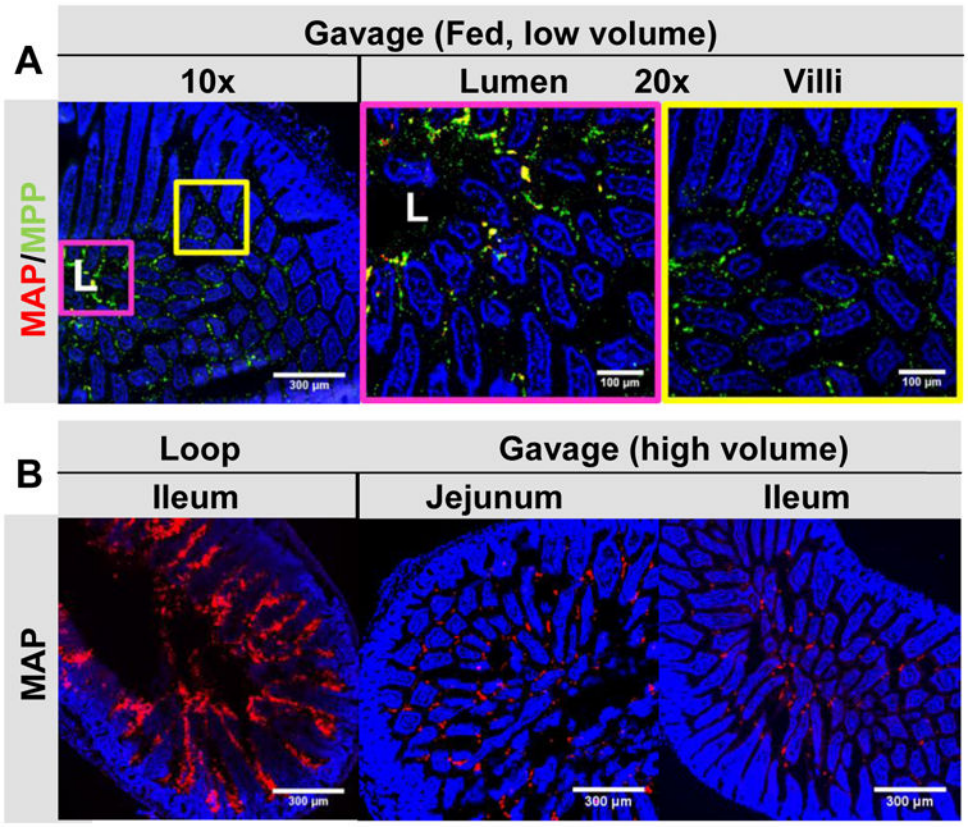

Figure 3. The impact of different experimental methods on the distribution of MAP and MPP in the jejunum and ileum

Distribution of fluorescent 200 nm MAP (red) or MPP (green) in: (A) the jejunum of healthy mice in the fed state after oral co-administration in a low volume gavage. In the 10× image, "L" denotes the lumen, the pink box outlines the luminal area (also shown outlined in pink at 20×), and the yellow box outlines the villi region (also shown outlined in yellow at 20×); and (B) the ileum of mice in the starved state after direct administration to an ileal loop, or in the jejunum and ileum after oral administration in a high volume gavage. Images are representative of $n \geq 3$ mice. White scale bars indicate 300 µm and 100 µm for 10× and 20× images, respectively.

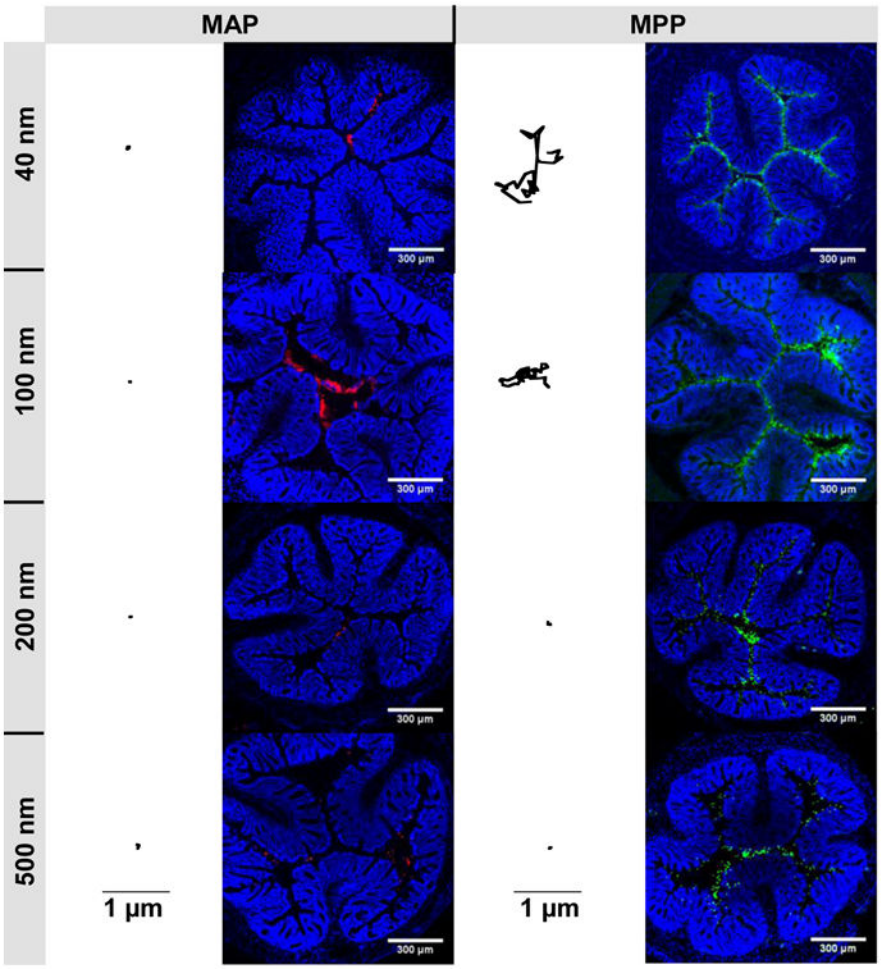

Figure 4. Trajectories in colorectal mucus and distribution of MAP and MPP in the mouse colorectum

Trajectories representative of 3 s of movement for 40, 100, 200, and 500 nm MAP and MPP in mucus on freshly excised mouse colorectal tissue. Black scale bars indicate 1 μm for all trajectories. Distribution in transverse colonic cryosections after rectal administration of 40, 100, 200, and 500 nm MAP (red) or MPP (green). Cell nuclei are stained with DAPI. White scale bars indicate 300 μm for all distribution images. Images are representative of $n \geq 3$ mice.

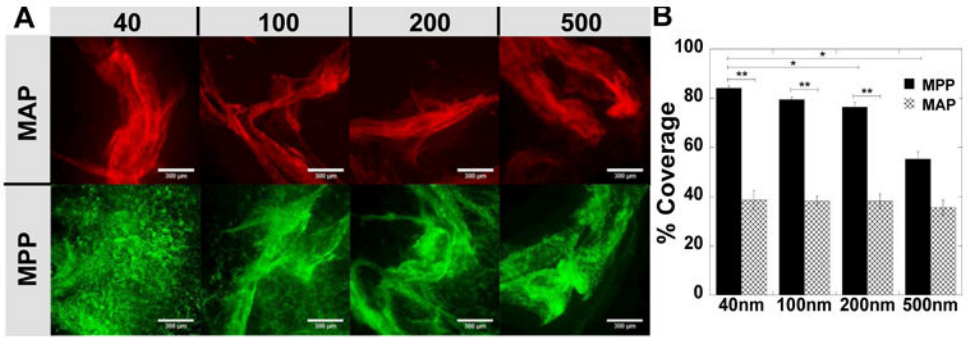

Figure 5. Quantified colonic distribution of MAP and MPP after rectal administration to mice

Distribution on flattened colonic tissue after rectal administration of 40, 100, 200, and 500 nm (A) MAP (red) or MPP (green). (B) Quantified surface coverage of various sized MAP and MPP on flattened mouse colonic tissue. Images are representative of n ≥ 3 mice and 6 images per tissue. White scale bars indicate 300 μm. Data are calculated as means ± SEM. **P* < 0.05 as compared to MAP, Student's t-test.

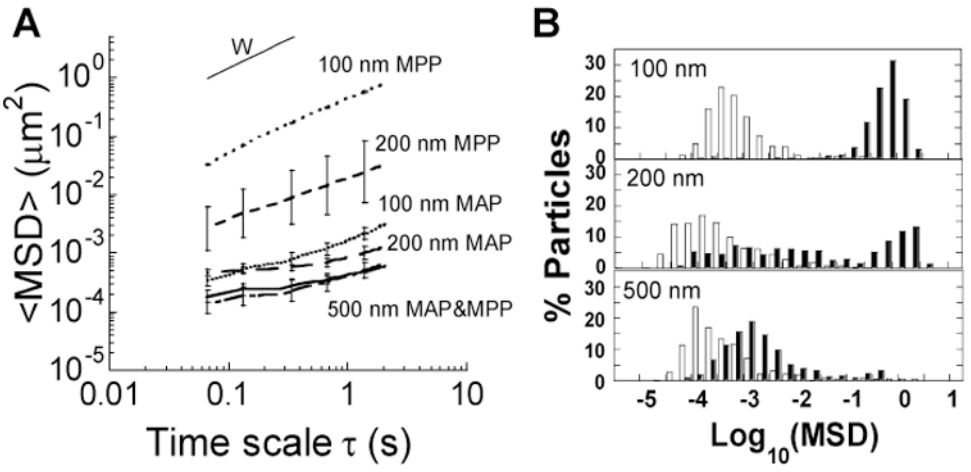

Figure 6. Transport of MAP and MPP in colorectal mucus on freshly excised *ex vivo* tissue from mice with TNBS-induced colitis

(A) Ensemble averaged mean-squared displacement (<MSD>) as a function of time scale for various sizes of MAP and MPP particles, including the theoretical MSD of 100 nm particles in water (W). (B) Distribution of the logarithms of individual particle MSD at a time scale of 1 s for various sized MAP (□) and MPP (■). Data is calculated as mean ± SEM (≥ 3 individual tissues with n > 100 particles per tissue).

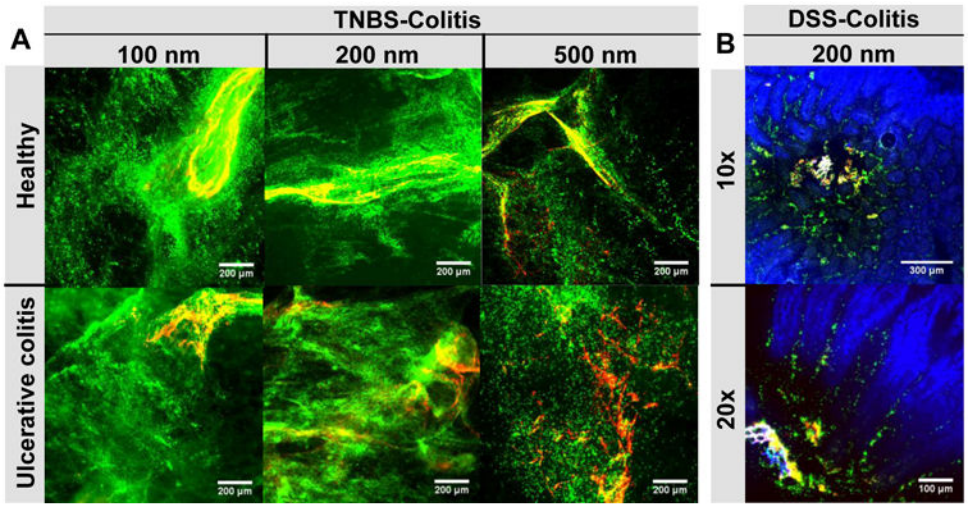

Figure 7. Distribution of various sizes of MAP and MPP after rectal co-administration to mice with TNBS-colitis and after oral co-administration to mice with DSS-colitis

Distribution of co-administered, fluorescent MAP (red) and MPP (green) (A) on flattened colonic tissue after rectal administration of various sizes (100 nm, 200 nm, 500 nm) to healthy mice and mice with TNBS-induced ulcerative colitis and (B) in the jejunum of mice with DSS-induced colitis after low volume oral co-administration of 200 nm particles (shown at 10× and 20× magnification). White scale bars indicate 200 μm in (A) and 300 μm for the 10× and 100 μm for the 20× images in (B). Cell nuclei are stained blue with DAPI. Images are representative of n ≥ 3 mice.

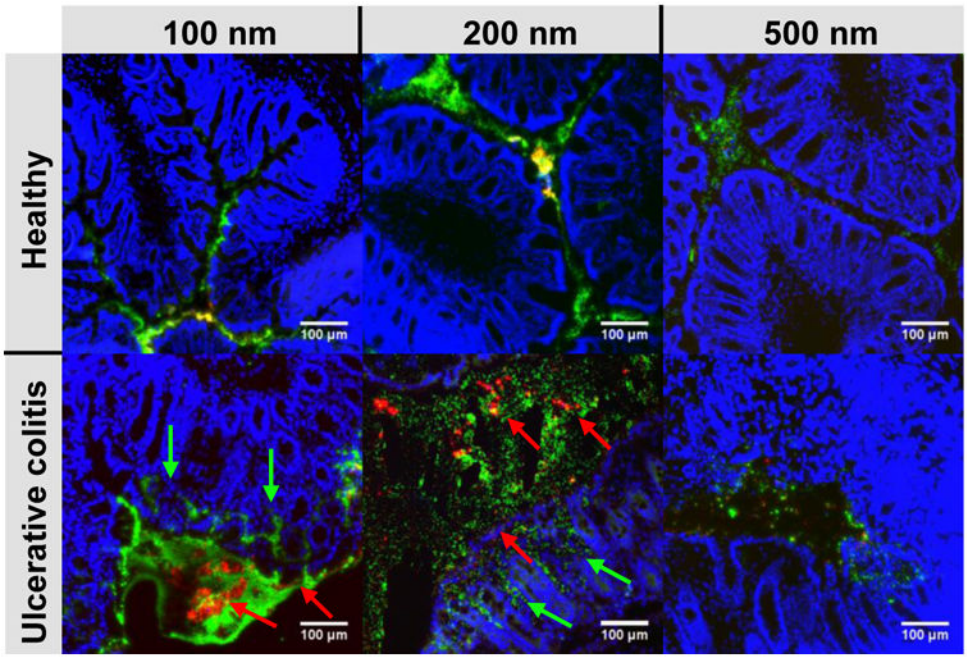

Figure 8. Distribution of various sizes of MAP and MPP after rectal co-administration to mice

Distribution of rectally co-administered, fluorescent MAP (red) and MPP (green) of various sizes (100 nm, 200 nm, 500 nm) in the colorectum of healthy mice and mice with TNBS-induced colitis. The red arrows highlight aggregates of MAP, while the green arrows highlight areas where the MPP have penetrated into the tissue. Cell nuclei are stained blue with DAPI. White scale bars indicate 100 μm. Images are representative of $n \geq 3$ mice.

Table 1

Comparison of ensemble averaged MSD of MPP in colorectal mucus from healthy mice and mice with TNBS-induced colitis. Values are representative of $n \geq 3$ mice. MSD_w denotes the theoretically diffusivity of similarly sized nanoparticles in water.

Particle Type	Healthy MSD_w/<MSD>	Colitis MSD_w/<MSD>	$MSD_{colitis}/MSD_{healthy}$
100 nm MPP	80	40	2
200 nm MPP	8000	300	25
500 nm MPP	24000	1900	13